

Transmission Electron Tomography 3D Reconstruction of Directed Self-Assembly Di-Block Copolymers

Gregory Pitner
Stanford University
Nanoelectronics Lab / EE367
gpitner@stanford.edu

Kye Okabe*
Stanford University
Nanoelectronics Lab
okabe@stanford.edu
*not in EE367

Abstract

The Directed Self-Assembly (DSA) technique using di-block copolymers is an emerging technology solution for the lithographic patterning of features below 10nm in future nanoelectronic fabrication processes. Creating 3-dimensional reconstructions of structures like DSA cells with nanometer-scale dimensions is extremely challenging, and requires specialized tools and resource-intensive sample preparation. In this work we present the first 3D transmission electron tomography of a DSA cell, and compare two reconstruction approaches: Inverse-Radon Filtered Back-Projection (FBP), and Landweber Simultaneous Iterative Reconstruction Technique (SIRT). The reconstruction has benefited researchers in this field due to the insight into of asymmetry in the cell and the 3-D sidewall profile.

1. Introduction

Directed Self-Assembly (DSA) is a technique in which di-block co-polymers are used to create nanometer-scale holes precisely positioned over a large area in a single processing step. This has great utility in nanoelectronics for defining features such as metal contacts to a state-of-the-art transistor. DSA is a significant improvement to traditional lithographic patterning, which is limited in resolution by the wavelength of light and is the most expensive component of modern fabrication flows. It is of great interest to researchers in this field to visualize the 3-dimensional structure of these DSA cells to communicate the profile and to investigate any common defects that may appear in the asymmetry of the cell.

To create 3-D nanometer-scale reconstructions is particularly challenging due to extreme requirements in resolution. Only one tool, an aberration-corrected Transmission Electron Microscope (TEM), can generate images with sub-nanometer resolution in ideal imaging conditions with ideal samples. This work uses a TEM to capture projections through the carefully prepared DSA sample. A series of single-axis tilts generated enough projections to enable a computational reconstruction of the 3-D DSA cell using TEM Tomography. More than one reconstruction technique is implemented and compared.

The final reconstruction is analyzed and displayed in several different ways to the benefit of researchers.

1.1. DSA Background^{1,2}

Directed-self Assembly, or DSA, is a technique in which a polymer with two blocks “A” and “B” (typically some derivative of Polystyrene and Poly(methyl methacrylate) (PMMA) are coated onto a wafer intended for fabricating small features such as transistor contacts. The wafer would typically contain some trenches or sidewalls that guide the polymer into a specific shape. Next, the substrate is heated until some critical temperature $\sim 100^{\circ}\text{C}$ in which the polymer would re-arrange itself into its minimum energy shape in which polymer end “A” would prefer to be with other “A” and polymer “B” would prefer to be with other “B”. Several possible shapes can be formed, but the process has been specially tuned to produce a circular pattern with holes with minimum dimensions on the order of 20nm or below, as shown in Figure 1d. The position of the holes is tightly controlled by the trench pattern on the substrate to match the desired layout determined by the circuit and application as shown in Figure 1a-c. By removing the central polymer circle, it is possible to position metal for contacts structures or etch down into the substrate using

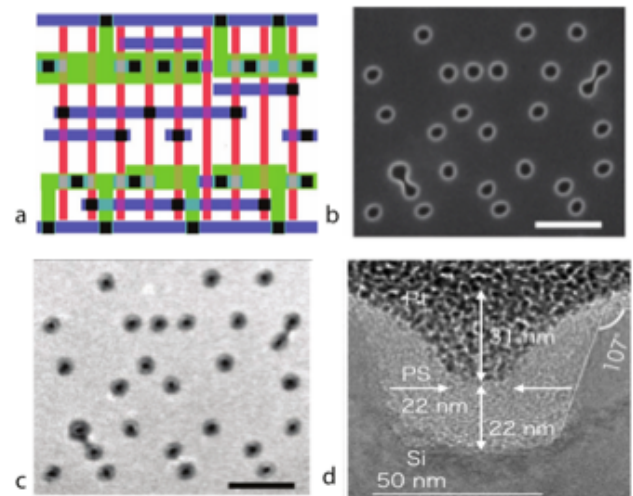


Figure 1: a) Typical VLSI standard cell layout. b) Guiding template. c) Guiding template filled with DSA pattern. d) Cross section SEM of DSA cell showing 22nm dimension.

the polymer “B” as a processing mask.

1.2. TEM Background

TEM imaging is a process in which a beam of high-energy electrons are focused by magnetic lenses onto an extremely thin sample and pass through to be captured by a charged-coupled device imager on the other side. The interaction of the electron beam with the sample can reveal features with angstrom-level resolution under ideal conditions. However, TEM requires very stringent sample preparation in order to achieve high-resolution results. Essentially, the sample must be thin enough for the beam of electrons to pass through, interacting only with the feature of interest. While not the focus of this work, the difficult sample preparation is one reason why a 3D reconstruction of this structure has not been achieved before. A second reason TEM 3D reconstruction is limited in its ubiquity is the intrinsic aberrations present in all but the highest-end TEM tools, one of which has been installed at Stanford University within the past 10 years.

A brief description of the TEM sample preparation is as follows: Beginning with a wafer containing an array of DSA contact holes, first the PMMA is removed and the substrate is coated with Platinum in the region of interest to protect it from damage and provide contrast in the hole. Then in a focused ion-beam tool (FIB), a trench is etched on either side of the feature of interest then narrowed until the remaining material is barely wider than the feature of interest, sub-100nm. A very fine probe tip is precisely bonded to the narrow trench using an electron-beam induced platinum chemical vapor deposition, which will

support the fin in the following steps. The remaining ends and bottom of the feature and fin are etched away with the FIB until the feature and fin are supported only by the probe tip, and it is lifted up and removed from the sample. This very thin fin is then placed on an ultra-thin TEM grid that is designed for the TEM sample stage and contains transparent windows for the electron beam to pass through the sample un-impeded. Now the TEM grid and sample are ready to be imaged. Once in the TEM chamber at a high vacuum level, the beam is aligned for focus, stigmation, and corrected for many different lens alignments and aberrations. A TEM overview figure is included in the supplementary figures in the submission folder. An example of the images captured at various angles are shown in figure 2 below, and a supplemental video containing all of these images is included with this submission with the name “Raw_Captured_TEMs_-68to+70.avi”.

2. 3D Reconstruction

Multiple 3D tomographic reconstruction techniques exist with tradeoffs including complexity, computation time, and noise characteristics. Gaussian thermal noise and Poisson shot noise is intrinsic in captured TEM images, and can lead to poor results if not addressed in the reconstruction. Missing projection wedges and imperfect alignment of the captured projections must also be addressed in the image processing pipeline. In this work we are reconstructing a single-axis tilt projections of the DSA cell into a 3D reconstruction. However, we find it convenient to consider each reconstructed plane separately since the final stack of 2D reconstructions results in a 3D structure. Therefore each 2D reconstruction can be reconstructed from a set of 1D slices from each level of the captured projections. This simplifies the implementation of the reconstruction substantially.

The image processing pipeline summary is shown in the figure 3 below. First, the raw captured TEM images were aligned using cross-correlation to correct for misalignment and thermal or charging drift that inevitably occurs during imaging. Next, the aligned images are reconstructed using one of two different reconstruction techniques. In this work, we utilize an inverse Radon transform implementation of the Filtered Back Projection (FBP) in the first case, and in the second case we use a Landweber variant of the Simultaneous Iterative Reconstruction Technique (SIRT). Finally the reconstructions are prepared for display by thresholding values and generating iso-surfaces. Each of these steps and their results will be described in detail in the following sub-sections.

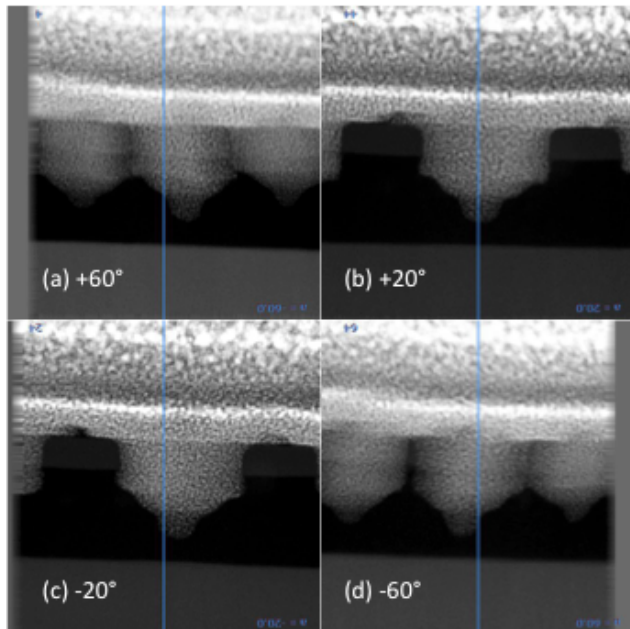


Figure 2: Examples of the captured TEM projections of DSA cells from -68° to $+70^\circ$ at increments of 2° between images for a total of 69 projections. The tip of the cell is less than 20nm.

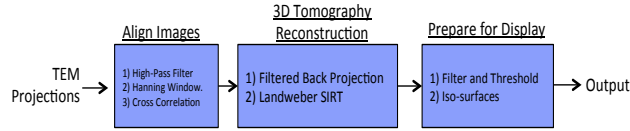


Figure 3: Image Processing Pipeline.

2.1. Image Alignment

The first step in the image processing pipeline is the alignment of the captured projections through a technique known as cross-correlation. The video containing the raw captured projections in the supplementary information illustrates clearly the presence of unwanted translation or drift due to mechanical, thermal and electrical charging induced vibrations on the sample. The projections can be aligned through a technique known as cross-correlation. First, a high-pass filter is applied to the images to emphasize the sharp edges. Next, the images pass through a hamming filter that washes out the periphery and prioritizes the feature of interest in the center. Then the images are shifted in x- and y-axis until the maximum correlation between the layers is observed. The calculated shifts are then applied to the original projections. This cross-correlation alignment is repeated using neighboring images until the alignment appears satisfactory by visual inspection. In this work, we aligned the images in 3 iterations before manually touching up any remaining errors. The final result is included in a supplementary video “3xAligned_Captured_TEMs_-68to+70.avi”. This cross-correlation was performed in a software tool provided by the TEM manufacturer FEI called Inspec.

2.2. Inverse Radon Filtered Back Projection

The 2D Radon transform is the integral of the projected density of function $f(x)$ over a projection line perpendicular to a range of projection angles, as described by eq. 1 below:

$$\mathcal{R}f(p, \hat{n}_\Omega) = \int_A f(x) \delta(p - x \cdot \hat{n}_\Omega) d^2x$$

Equation 1: 2D Radon Transform.

The result from this transform is a sonogram of projection intensities along this projection line versus the projection angles through the 2D structure. The key feature of a 2D radon transform is that, much like a Fourier transform, it is highly invertible. This invertibility allows us to reconstruct the initial 2D function using only single-axis tilt projection data captured for many angles from the TEM.

Essentially, we take a single pixel line at the same z-height from each angled projection and construct a sonogram, as shown in Figure 4a and 4b below. Then we apply the inverse radon transform in order to re-create the

2D structure from the 1D projection. By reconstructing a 2D plane for each z-axis plane we are able to stack the planes and re-create the 3D structure. One final detail of importance is that each projection angle is essentially a ray through the origin in Fourier space. Therefore, it becomes important to filter the projection data with a high-pass filter to weight the higher frequencies. This work uses a Ram-Lak filter. A comparison of non-filtered and filtered reconstructions is shown in the figure 4c-d below. The filtered back-projection clearly resolves the DSA cell, and even reveals a slight non-uniformity. In our estimation, the flat edge is due to an error when thinning the sample during preparation, and not an intrinsic DSA flaw. This reconstruction technique was implemented in Matlab.

The final reconstruction from the Inverse Radon Filtered Back Projection for all layers is included in several supplementary videos with this submission. The video “RadonFBP_3DTopView_FullFrame” starts at $z=0$ and displays increasing height until reaching the top of the reconstruction at $z=512$, while the highlight version of the video focuses on the structure of interest. Likewise, the video “RadonFBP_3DSideView_FullFrame” starts at $y=0$ and displays deeper until reaching the end of the reconstruction at $y=512$, while the highlight version of the video focuses on the structure of interest.

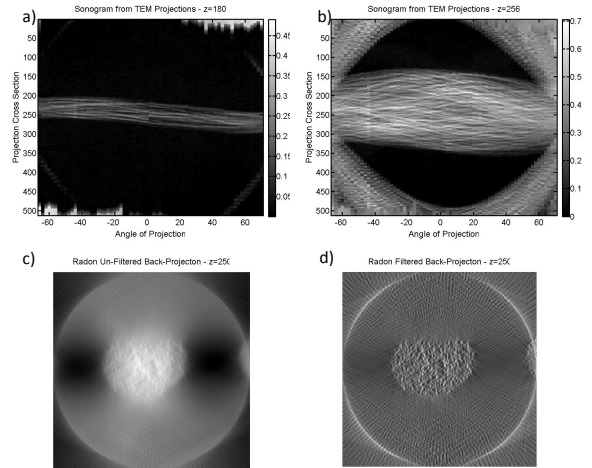


Figure 4: a) Sonogram of cross-section vs. angle for $z=180$. b) Sonogram at $z=256$. c) Radon reconstruction with no high-pass filter showing low-frequency noise. d) Radon reconstruction with Ram-Lak high-pass filter showing much better noise characteristics than (c)

2.3. SIRT Reconstruction³

The simultaneous iterative reconstruction technique, or SIRT, is another option for reconstructing projections. In this approach the forward problem of obtaining the projections is considered a matrix multiplication:

$$Ax = b$$

Equation 2: Matrix formulation of projection.

in which ‘x’ is the original structure with dimensions N^2 rows by 1 column ($N \times N$ being the original dimensions of the projection). ‘A’ is a projection matrix with dimensions $p \times nA$ rows by N^2 columns (p being the number of projection rays and nA being the number of projection angles), which describes the path of the projections through the N by N structure. ‘b’ describes the resulting projection information with dimensions $nA \times p$ rows by 1 column. Therefore we would like to solve the inverse matrix problem starting with the projection information contained in ‘b’. However, this is an ill-posed problem considering the noise, misalignment, missing angle and other imperfections intrinsic in the captured projections that make any direct 1-step reconstruction very poor.

Therefore the SIRT technique uses iteration to determine the inverse problem’s solution:

$$x^{k+1} = x^k + \lambda_k A^T (b - Ax^k)$$

Equation 3: Classic Landweber SIRT Formulation.

Where x^k is the current solution (for iteration $k=0$, assume array of zeros), x^{k+1} is the next solution, A and A^T are the projection matrix and transposed projection matrix, b is the projection data, and λ is a relaxation parameter computed each step to satisfy λ less than the reciprocal of the maximum singular value of the matrix A . Increasing the number of iterations, k , can improve the noise behaviors of the final solution but makes the computation take longer.

The TEM projections are first manipulated to generate the array ‘b’ for each z-slice through the structure. Next, the array A is created for each projection from each angle with help from a matlab script package AIR tools created by researchers at the Technical University of Denmark in 2014 that can simulate projections from parallel-beam topographies. The reconstruction is calculated for a range of iteration values at each vertical slice through the structure. During later trials we imposed a constraint on each iteration that the solution could not be negative. The reconstruction was calculated using an AIR tools implementation of the Landweber formulation in matlab.

To investigate the effect of iteration value on the solution, one z-cross section reconstruction was simulated at k values from 1 to 150, as shown in the figure 5 below and the included supplementary video “SIRT_IterationEffect_FullFrame.avi”. An optimum value was observed somewhere between $k=30$ and $k=80$ iterations. As the iterations increased the reconstructions contained less projection noise but the central feature lost its contrast. It is also worth noting a significant (roughly linear) increase in the computation time required to perform more SIRT iterations.

The reconstruction of the entire structure was completed for $z=1$ through $z=512$ for iterations of $k=30$ and $k=80$. Both final reconstructions are reported in the videos “SIRT_ZCrossSection_30Iter_FullFrame.avi” and “SIRT_ZCrossSection_80Iter_FullFrame.avi” included

with the supplementary information. The best result includes the nonnegative constraint for 30 iterations and is entitled “BEST RESULTS -SIRT_ZCrossSection_30IterNonneg_FullFrame_Highlights.avi”.

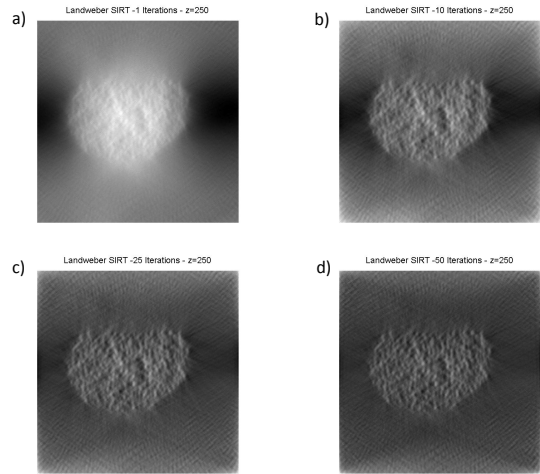


Figure 5: Effect of SIRT iterations on resulting reconstructions. a) 1 iteration, b) 10 iterations, c) 25 iterations, d) 50 iterations. An optimum was found between 30 and 80 iterations. For higher iterations up to 150 the reconstructed region became somewhat fainter as the signal decreased gradually.

2.4. Comparison between FBP and SIRT

The two approaches to reconstructing the DSA cell, Radon FBP and Landweber SIRT, are expected to deliver different capabilities for reconstruction speed and noise characteristics. In particular, FBP is expected to be significantly faster reconstruction while SIRT is expected to have lower noise after many iterations. In the table 1 below, the values for simulation speed are tabulated for FBP and SIRT with $k=30$ and $k=80$. It can be seen that SIRT takes 300-600x, more than 2 orders of magnitude, as much time to simulate a single 2-D reconstruction. In practice, one attempt reconstructing a complete 3-D structure took up to 2 hours using SIRT, which is one disadvantage and does not scale well to larger structures with higher resolution or more iterations.

Table 1: Simulation time to reconstruct a single z-cross section comparison between FBP and SIRT. Each time value is an average from >150 2-D reconstructions.

	<i>FBP</i>	<i>SIRT k=30</i>	<i>SIRT k=80</i>
Time (sec)	0.023	6.75	12.86

The figure 6 below shows a side-by-side comparison of the reconstruction outputs for several cross sectional heights, drawing attention to the different noise characteristics. Each of these images has had the data values scaled to the maximum range for the colormap in

order to maximize contrast, but image processing that would manipulate the output data values, e.g. changing the gamma values, have deliberately not been implemented. It can be seen that the SIRT reconstructions have much better characteristics regarding radial projection noise (the radial streaks originating from the DSA structure) and lower background levels than the FBP. In addition, due to the formulation of the matrix A the SIRT reconstructed volume focuses on the pixels of the feature of interest rather than the larger projection, as compared to the larger pseudo-resolution as seen in FBP. This is what causes the imaginary perimeter rings seen in the FBP reconstructions. Finally, the FBP actually displays a higher signal level than SIRT, indicating that some signal is lost during the convergence of SIRT. This is supported by the observation that with increasing iterations k up to 150, the signal from the feature of interest decreases until it is nearly invisible against the background. Ultimately, the SIRT technique with optimal iteration provides the better reconstruction results of the two.

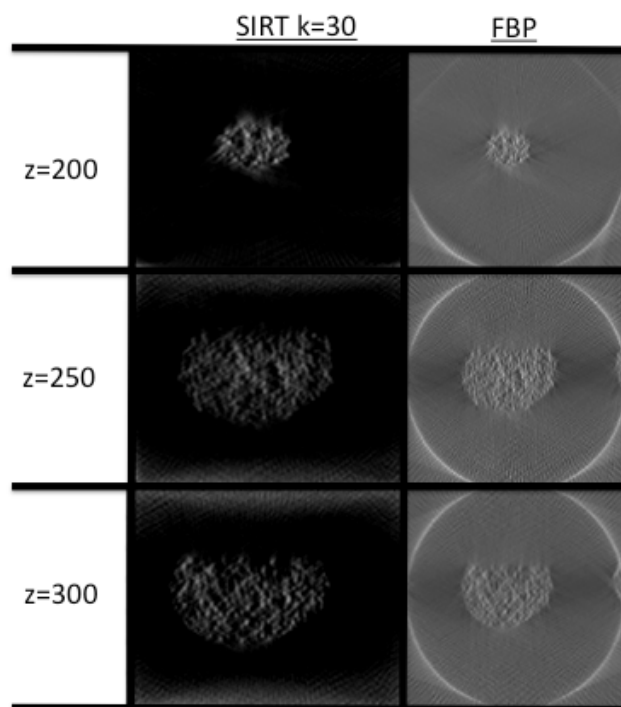


Figure 6: Comparison between SIRT and FBP. SIRT examples use 30 iterations with non-negativity constraint at each iteration, and display better lower noise characteristics in the region in which no structure should be visible. However, FBP has a higher signal level.

2.5. Final reconstruction

The third phase of the tomography processing pipeline is to process the data in a way that makes it suitable for display. The approach we use is to threshold the data

values then generate iso-surfaces at that threshold value. These surfaces, if chosen appropriately, can give a very reasonable depiction of the DSA morphology, and deliver on the goal of revealing the 3D structure of the cell.

In matlab, the best reconstruction (SIRT with nonnegativity constraints) was cropped to the approximate rectangular volume of interest, and then thresholded for display using the isosurface command. Increasing threshold values yielded values with varying depth within the structure, as expected. The figure 7 below displays the reconstructions from several angles. The reconstructions are also included in a video⁴ in the supplementary information entitled “IsoSurfacePan_30kNonNeg_001Threshold.mp4”, “IsoSurfacePan_30kNonNeg_0025Threshold.mp4” and “IsoSurfacePan_30kNonNeg_0045Threshold.mp4”.

As can be seen, the profile of the DSA cell is revealed. In particular, we observe the distinct 3D sidewall profile, elliptical asymmetry, and even some flattening damage induced on one side of the cell during the sample preparation.

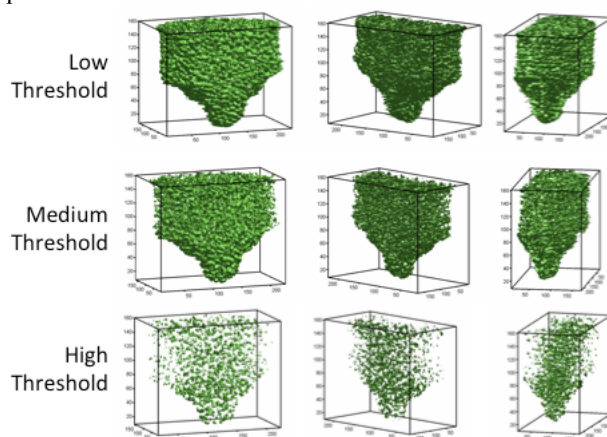


Figure 7: The reconstructions have been thresholded to create iso-surfaces for 3-D display.

3. Conclusion

This work revealed for the first time the 3 dimensionality of a directed self-assembly di-block copolymer cell. By careful sample preparation and transmission electron microscopy, we were able to capture a range of single-axis tilt projections of the DSA cell. With this projection data set we implement cross-correlation alignment, two different tomographic reconstruction algorithms including the superior SIRT algorithm, and an isosurface reconstruction for display. Researchers in nanoelectronics lithography and devices would certainly be interested to see, for the first time, the 3D profile of this DSA cell that will be used to create state-of-the-art nanometer-scale features in electronics in the very near future.

For future work, the reconstruction results could likely

be enhanced by including weighting using priors in the reconstruction algorithm that account for the relative absorption of the different materials in the DSA cell.

References

- [1] H. Yi, X.-Y. Bao, R. Tiberio, H.-S. P. Wong, “Design Strategy for Small Topographical Guiding Templates for sub-15 nm Integrated Circuits Contact Hole Patterns using Block Copolymer Directed Self-Assembly,” *Proc. SPIE* 8680, Alternative Lithographic Technologies V, 868010, (2013).
- [2] K. Okabe, H. Yi, M. Tung, R. Tiberio, J. Bekaert, R. Gronheid, H.-S. P. Wong, “Cross-sectional Imaging of Directed Self Assembled Block Copolymers,” *Proc. SPIE* 9423, Alternative Lithographic Technologies V, 9423-43, (2015).
- [3] P. C. Hansen, M. Saxild-Hansen, “AIR Tools MATLAB Package of Algebraic Iterative Reconstruction Techniques – version 1.2”, Dept. of Applied Mathematics and Computer Science, Technical University of Denmark, Lyngby Denmark. 2014.
- [4] Alan Jennings, “CaptureFigVid Matlab Script” – Aeronautics and Astronautics, Air Force Institute of technology,

Author Contributions

Kye Okabe prepared the DSA sample and captured a set of TEM projections for his original research published in reference 2. Gregory Pitner implemented a 3D reconstruction pipeline.